

# Preliminary Results of NASA's First Autonomous Formation Flying Experiment: Earth Observing-1 (EO-1)

David Folta  
NASA/Goddard Space Flight Center  
Greenbelt, MD

Albin Hawkins  
a.i.-solutions  
Lanham, MD

## ABSTRACT

NASA's first autonomous formation flying mission is completing a primary goal of demonstrating an advanced technology called enhanced formation flying. To enable this technology, the Guidance, Navigation, and Control center at the Goddard Space Flight Center has implemented an autonomous universal 3-axis formation flying algorithm in executive flight code onboard the New Millennium Program's (NMP) Earth Observing-1 (EO-1) spacecraft. This paper describes the mathematical background of the autonomous formation flying algorithm and the onboard design and presents the preliminary validation results of this unique system. Results from functionality assessment and autonomous maneuver control are presented as comparisons between the onboard EO-1 operational autonomous control system called AutoCon™, its ground-based predecessor, and a standalone algorithm.

## INTRODUCTION

With the launch of NASA's Earth Observer-1 satellite (EO-1), the Goddard Space Flight Center is demonstrating the capability of satellites to fly in formation, to react to each other, and maintain a close proximity without human intervention. This advancement allows satellites to autonomously respond to each other's orbit changes quickly and more efficiently. It permits scientist to obtain unique measurements by combining data from several satellites rather than flying all the instruments on one costly satellite. It also enables the collection of different types of scientific data unavailable from a single satellite, such as stereo views or simultaneously collecting data of the same ground scene at different angles.



Figure 1. EO-1 Formation Flying Behind Landsat-7

The need for an innovative technical approach to autonomously achieve and maintain formations of spacecraft is essential as scientific objectives become more ambitious.<sup>1,2</sup> The development of small low-cost spacecraft and new scientific research such as large scale interferometry has led many programs to recognize the advantage of flying multiple spacecraft in formation to achieve correlated instrument measurements. Advances in automation and technology by the Guidance Navigation and Control (GN&C) center at the Goddard Space Flight Center (GSFC) has resulted in the development and demonstration of an autonomous system to meet these new guidelines.

The EO-1 technology incorporates the Folta-Quinn (FQ) 3-axis universal algorithm for formation control. This system can be used by single spacecraft or spacecraft in constellations and formations. It can also be applied to Low Earth Orbits, Highly elliptical orbits, and non-keplerian trajectories such as libration orbits. The system allows the burden in maneuver planning and execution to be placed onboard the spacecraft, mitigating some of the associated operational concerns while increasing autonomy.

The EO-1 formation flying requirements on our technology are to demonstrate the capability of EO-1 to fly over the same groundtrack as Landsat-7 within  $\pm 3$  kilometers at the equator while autonomously maintaining the formation for extended periods to enable paired scene comparisons between the two satellites. The required relative separation is 1 minute in mean motion, equivalent to 450km. The tolerance on this separation to meet the ground track is  $\pm 6$  seconds, or roughly 42 km.

This paper presents preliminary validation results of formation flying of the NMP EO-1 spacecraft with respect to the Landsat-7 spacecraft. Results are presented as comparisons between the onboard autonomous formation flying control system and two ground systems. Both the onboard and the prime ground systems use AutoCon™ a high fidelity modeling package which incorporates the FQ Algorithm. This overall NMP autonomous control experiment is called Enhance Formation Flying (EFF).

## **FORMATION FLYING**

Formation flying involves position maintenance of multiple spacecraft relative to measured separation errors. For EO-1, this relative separation between the EO-1 and Landsat-7 spacecraft is required to allow co-scene comparisons. An overview of the EO-1 formation flying using a two spacecraft differential drag example is presented here.

### **Mechanics Using Differential Drag**

If two spacecraft are placed in similar orbital planes and similar altitudes with a small initial separation angle they will be equally affected by the Geopotential field of the Earth and by atmospheric drag provided that they have identical ballistic properties. As long as the separation angle is small enough that atmospheric density and gravitational perturbations can be considered constant, the relative separation will remain the same. If the spacecraft are separated in the radial direction, and the respective ballistic properties are different, their orbit velocities are also different, and one spacecraft (the EO-1 / chase spacecraft) will appear to drift relative to the other (Landsat-7 / control spacecraft). The drifting is most apparent in the along-track (orbital velocity) direction. The radial separation can be operationally planned or induced by differential decay rates caused by environmental perturbations. The concept of formation flying for EO-1 is based on the constructive use of the differential decay rates as a direct function of differential ballistic properties between a reference and a free-flying spacecraft.

### **EO-1 Example**

An example of the orbit dynamics of EO-1 and Landsat-7 formation flying is shown in Figure 2. In the figure, EO-1 starts a formation at the red dot location, behind Landsat-7 by 450 kilometers and above by  $\sim 50$  meters. Due to the differences in the drag accelerations from the atmosphere, the EO-1 orbit decays slightly faster. While above Landsat-7, EO-1 is drifting away from Landsat-7 since the average orbital velocity is less than that of Landsat-7. After several days of orbital decay due to atmospheric drag EO-1 will be below Landsat-7 and will drift towards

Landsat-7 since the average orbital velocity is now higher than that of Landsat-7. When EO-1 is outside the required tolerance box or if Landsat-7 has maneuvered, EO-1 will autonomously compute and perform a maneuver to reposition it to an initial condition to repeat the relative motion.

### FORMATION FLYING ALGORITHM

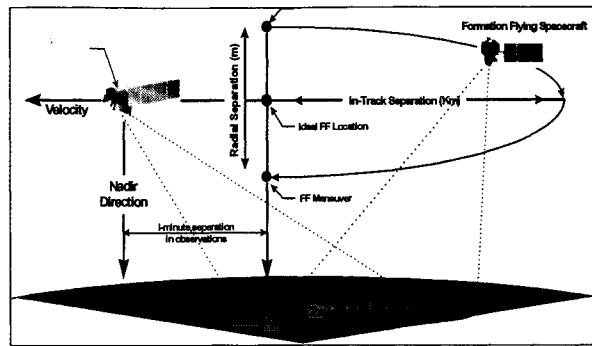


Figure 2. EO-1 Formation Flying Using Differential Drag

The Folta-Quinn (FQ) algorithm is a new technology that is based on mathematics derived by Battin and adapted to the formation flying problem.<sup>3,4</sup> A patent application has been submitted to the GSFC Office of Patent Counsel for the application of Autonomous Closed Loop 3-Axis Navigation Control Of Spacecraft<sup>5</sup>. This patent-pending technology will allow full closed-loop maneuver autonomy onboard any spacecraft rather than the tedious and costly operational activity historically associated with ground based operations and control. The application to other missions is unlimited and can therefore be used to more fully explore the NASA mandate of faster, better, cheaper spacecraft.

### FQ Algorithm Description

The FQ algorithm for formation flying solves the position maintenance problem by combining a modified Lambert's two point boundary value problem and Battin's 'C\*' matrix with an autonomous system developed by a.i.-solution, Inc. of Lanham MD. called AutoCon™. The algorithm enables the spacecraft to execute complex three axis orbital maneuvers autonomously. Figure 3 illustrates the basic sets of information required for the EO-1 formation targeting as it is incorporated into AutoCon™. The FQ algorithm well is suited for multiple three axis burn scenarios but is more easily explained using a two-burn, co-planar example for clarity.

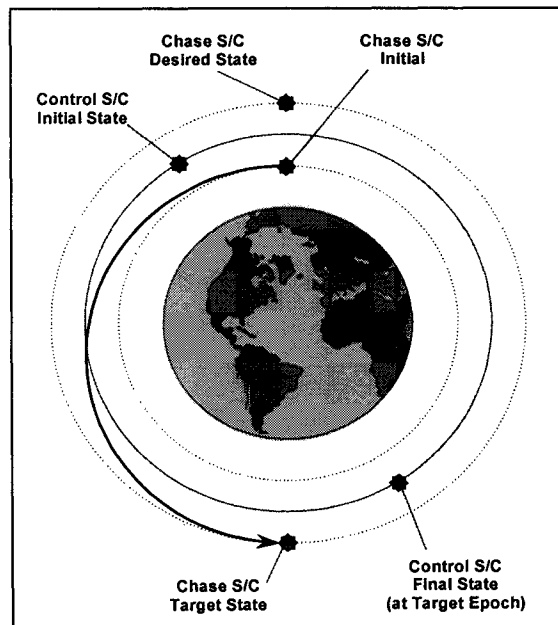


Figure 3. FQ Algorithm Inputs for EO-1 Formation Flying

The formation flying problem in this example involves two spacecraft orbiting the Earth. Landsat-7, the control spacecraft, orbits without performing any formation flying maneuvers. EO-1, the chase spacecraft monitors the control spacecraft, and performs maneuvers designed to maintain the relative position imposed by the formation requirements. In this example, the goal of the formation flying algorithm is for EO-1 to perform maneuvers which cause it to move along a specific transfer orbit. The transfer orbit is established by determining a path (in this case a Keplerian path) which will carry the EO-1 spacecraft from some initial state,  $(\mathbf{r}_0, \mathbf{v}_0)$ , at a given time,  $t_0$ , to a target state,  $(\mathbf{r}_t, \mathbf{v}_t)$ , at a later time,  $t_t$ . The target state is found to be one which will place EO-1 in a location

relative to Landsat-7 so as to maintain the formation. A desired state is also computed. This is accomplished by back propagating the target state to find the initial state that EO-1 would need at time  $t_0$  for it to achieve the target state at time  $t_1$  without executing a maneuver. This back propagation of the target state gives rise to the desired state,  $(r_d, v_d)$  at time  $t_0$ . The initial state can now be differenced from the desired state to find:

$$\begin{pmatrix} \delta r \\ \delta v \end{pmatrix} = \begin{pmatrix} r_0 - r_d \\ v_0 - v_d \end{pmatrix}$$

### STM Formulation

The FQ Algorithm uses state transition matrices, described below, for the calculation of the maneuver  $\Delta V$ . Selecting initial conditions prescribed at a time  $t_0$  so that the state at this time has all zero components except the  $j$ th term which is unity, a state transition matrix,  $\Phi(t_1, t_0)$ , can be constructed such that it will be a function of both  $t$  and  $t_0$  and satisfies matrix differential equation relationships<sup>5</sup>. The initial conditions of  $\Phi(t_1, t_0)$  are the identity matrix.

Having partitioned the state transition matrix,  $\Phi(t_1, t_0)$  for time  $t_0 < t_1$ ,

$$\phi(t_1, t_0) \equiv \begin{bmatrix} \phi_1(t_1, t_0) & \phi_2(t_1, t_0) \\ \phi_3(t_1, t_0) & \phi_4(t_1, t_0) \end{bmatrix}$$

We find the inverse may be directly obtained by employing symplectic properties

$$\phi^{-1}(t_1, t_0) \equiv \phi(t_0, t_1) \equiv \begin{bmatrix} \phi_1(t_0, t_1) & \phi_2(t_0, t_1) \\ \phi_3(t_0, t_1) & \phi_4(t_0, t_1) \end{bmatrix}$$

$$\phi^{-1}(t_1, t_0) \equiv \begin{bmatrix} \phi_4^T(t_1, t_0) & \phi_2^T(t_1, t_0) \\ \phi_3^T(t_1, t_0) & \phi_1^T(t_1, t_0) \end{bmatrix}$$

Where the matrix  $\Phi(t_0, t_1)$  is based on a propagation forward in time from  $t_0$  to  $t_1$  and is sometimes referred to as the navigation matrix, and  $\Phi(t_1, t_0)$  is based on a propagation backward in time from  $t_1$  to  $t_0$ , and is sometimes referred to as the guidance matrix. We can further define the transition matrix partitions as follows:

$$\begin{aligned} \tilde{R}^*(t_0) &\equiv \phi_1(t_0, t_1) & \tilde{R}(t_1) &\equiv \phi_1(t_1, t_0) \\ R^*(t_0) &\equiv \phi_2(t_0, t_1) & R(t_1) &\equiv \phi_2(t_1, t_0) \\ \tilde{V}^*(t_0) &\equiv \phi_3(t_0, t_1) & \tilde{V}(t_1) &\equiv \phi_3(t_1, t_0) \\ V^*(t_0) &\equiv \phi_4(t_0, t_1) & V(t_1) &\equiv \phi_4(t_1, t_0) \end{aligned}$$

Substituting yields the following useful identities:

$$\begin{bmatrix} \tilde{R}^*(t_0) & R^*(t_0) \\ \tilde{V}^*(t_0) & V^*(t_0) \end{bmatrix} = \begin{bmatrix} V^T(t_1) & -R(t_1) \\ -\tilde{V}^T(t_1) & \tilde{R}(t_1) \end{bmatrix}$$

Where the starred quantities are based upon a guidance matrix and unstarred quantities are based on a navigation matrix. If a reversible Keplerian path is assumed between the two states, one should expect the forward projection of the state from  $t_0$  to  $t_1$  to be related to the backward projection of the state from  $t_1$  to  $t_0$ . When the fundamental matrices  $C$  and  $C^*$  are defined as

$$\tilde{C}^* \equiv \tilde{V}^* \tilde{R}^{*-1} \quad \text{and} \quad C^* \equiv V^* R^{*-1}$$

We find the following:

$$\tilde{C}^* \equiv \left. \frac{\partial v_0}{\partial r_0} \right|_{v_1 = \text{constant}} \quad \text{and} \quad C^* \equiv \left. \frac{\partial v_0}{\partial r_0} \right|_{r_1 = \text{constant}}$$

so that  $C \delta r = \delta v_0$  becomes the velocity deviation required at time  $t_0$  ( as a function of the measured position error  $\delta r$  at time  $t_0$ ) if the spacecraft is to arrive at the reference position  $r_1$  at time  $t_1$  (with arbitrary velocity). Recalling that the starred quantities were obtained based on the guidance matrix, the symplectic property allows them to be computed based on a navigation projection. It can therefore be shown that

$$[C^*(t_0)] = [V^*(t_0)] [R^*(t_0)]^{-1} = [\tilde{R}^T(t_1)] [-R^T(t_1)]^{-1}$$

Applying a universal variable formulation of the closed-form state transition matrix, the relevant state transition matrix submatrices are computed.<sup>4,5</sup> The expressions for  $F$ ,  $G$ ,  $F_t$  and  $G_t$  are derived from the Gauss problem of planar motion;  $K$  is a quantity derived from the Universal Variable (U) formulation.<sup>5</sup> These variables are dependent upon each other in their formulation, i.e.  $U(6)$  is dependent upon  $U(4)$  and on intermediate variables related to the classic  $f$  and  $g$  series. The target and desired states,  $r_d, v_d, r_t,$  and  $v_t$  are computed from the propagated states.  $\mu$  is the universal gravitational constant.  $R$  and  $\tilde{R}$  are then defined from the target and desired states as:

$$\begin{aligned} R(t_t) &= \frac{|r_d|}{\mu} (1 - F) [(r_t - r_d) v_d^T - (v_t - v_d) r_d^T] + \frac{K}{\mu} [v_t v_d^T] + G [I] \\ \tilde{R}(t_t) &= \frac{|r_t|}{\mu} [(v_t - v_d)(v_t - v_d)^T] + \frac{1}{|r_t|^3} [r_t (1 - F) r_t r_d^T + K v_t r_d^T] + F [I] \end{aligned}$$

From these variables and sub-matrices, the  $C^*$  matrix is computed as follows:

$$\begin{aligned} R^*(t_0) &= -R^T(t_t) \\ V^*(t_0) &= \tilde{R}^T(t_t) \\ C^*(t_0) &= V^*(t_0) [R^*(t_0)]^{-1} \end{aligned}$$

The expression for the impulsive maneuver follows immediately:

$$\Delta V = [C^*(t_0)] \delta r_0 - \delta v_0$$



## Formation Flying Control

The AutoCon™ flight control system ingest data from EO-1 sensors and subsystems such as propulsion, navigation, and attitude data. It then autonomously generates, analyzes, and executes the maneuvers required to initialize and maintain the formation between Landsat-7 and EO-1. Figure 5 shows a functional diagram of EFF and AutoCon™ system. Because these calculations and decisions are performed onboard the spacecraft, the lengthy period of ground-based planning currently required prior to maneuver execution will be eliminated. The system is general and modular so that it can be easily extended to future missions. Furthermore, the AutoCon™ flight control system is designed to be compatible with various onboard navigation systems (i.e. GPS, or an uploaded ground-based ephemeris). The AutoCon™ system is embedded in the Mongoose-5 EO-1 spacecraft computer. Interfaces are handled with one interface to the C&DH system. This is used for the ingest of GPS states information, AutoCon™ commanding, EFF telemetry, and maneuver commands for EO-1 as well. The FQ algorithm needs input data for the current EO-1 state, the target state, and the desired state. These data are provided by AutoCon™. AutoCon™ takes the current EO-1 and uploaded Landsat-7 states and then propagates these states for a user-specified fraction of the period. Autonomous orbit control of a single spacecraft requires that a known control regime be established by the ground which is consistent with mission parameters. That data must then be provided to the spacecraft. When orbital perturbations carry the spacecraft close to any of the established boundaries, the spacecraft reacts (via maneuver) to maintain itself within its error box. The system is currently set to check the tolerance requirements every 12 hours. From this point AutoCon™ propagates the states for 48 hours (a commandable setting) and will execute a maneuver plan if needed.

### Algorithm Modes

There are five EFF maneuver control modes onboard EO-1 as shown in Figure 6. The control modes verified during this preliminary validation process are modes 1, 2 and a partial of 3. These modes were established to allow an incremental validation of the system performance, data interfaces, and maneuver computations before commands were generated onboard for an executable maneuver.

### $\Delta V$ Computations and Quantized Maneuvers

The computation of the EO-1 maneuver  $\Delta V$ s is performed using a sequence of two methods.

The first method uses the FQ algorithm for the calculation of the maneuver to reach the targeted position relative to Landsat-7. Subsequently, a velocity-matching maneuver is then performed once the targeted position is attained. The FQ algorithm could also be used, but in an effort to conserve onboard resources a velocity matching method is employed. This velocity matching is computed from the difference in the velocity of the EO-1 transfer orbit and the targeted state

The EO-1 spacecraft propulsion system was designed so that the minimum maneuver duration is one second with larger burns selectable at one-second increments. This means that commands generated either onboard or on the ground will undergo a rounding of the maneuver duration based on the computed  $\Delta V$ . For example if a maneuver is such that the computed maneuver duration is 5.49 seconds, the commanded maneuver will actually be 5 seconds, and a 5.51 second

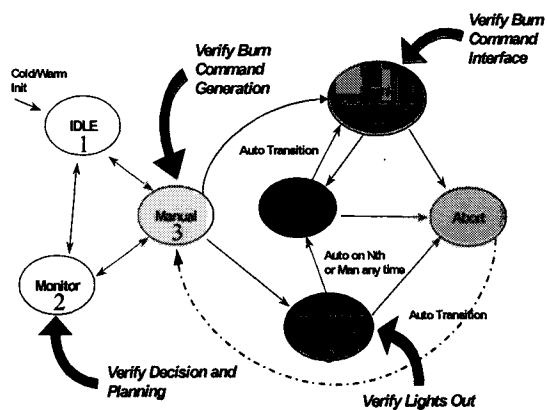


Figure 6 EFF Maneuver Modes

duration would become 6 seconds. This results in a quantized maneuver duration for each maneuver and thus the achieved Keplerian trajectory will differ slightly from the targeted trajectory. To compensate for this effect the final  $\Delta V$  is adjusted. The velocity match is perturbed slightly to compensate for the position error resulting from the prior maneuver's quantized burn duration. This allows the targeted orbit's SMA to be achieved with a trivial sacrifice of eccentricity.

## **PRELIMINARY VALIDATION RESULTS**

On January 12, 2001, the Enhanced Formation Flying (EFF) Experiment onboard EO-1 became operational. EFF was started in the modes 1 and 2 whereby GPS data would flow through the C&DH interface into the AutoCon™ executable and maneuvers were computed continuously. Scripts and data uploaded via tables were enabled through the execution of EFF. With this data maneuvers were calculated at specified intervals. The overall computational interval was approximately 3 hours in duration and began with the ingest of a single GPS EO-1 state. This state, along with an uploaded Landsat-7 State, was then propagated onboard for durations of 12 hours, 24 hours, and 48 hours. Maneuvers were computed at the 12, 24, and 48 hour epoch marks. After the last maneuver was computed, a new GPS EO-1 state was ingested and the process began again. This enabled the continuous computation of maneuvers while verifying the ingest and data interfaces and propagation of states onboard EO-1.

### **Validation Results and Period of Performance**

This EFF script ran over a several week period, Jan 12 through February 10, and generated over 530 maneuver plans. These maneuvers were planned in sets of three based on the three propagation durations. GPS data was ingested 177 times while tables were uploaded approximately 30 times for script control, Landsat-7 data, and environmental data updates. The preliminary validation was accomplished by looking at several events and computations. These included:

- EO-1 GPS and Landsat-7 state ingest
- EO-1 and Landsat-7 Propagation Events (Target and Desired States)
- Folta-Quinn Targeting Algorithm Output
  - ◆ Quantized Maneuver  $\Delta V$
  - ◆ 3-D maneuver  $\Delta V$
  - ◆ Internal Calculations (Matrices, Variables, States)

### **EO-1 Relative Motion**

The following results are comparisons taken directly from the EO-1 playback telemetry which provides the output from the onboard EFF AutoCon™ flight code to the output of using the playback states as input to the PC AutoCon™ ground system and the original MATLAB FQ algorithm. The Landsat-7 initial orbit conditions were taken from the playback telemetry. The Landsat-7 states uploaded for the test were obtained from the Landsat-7 project. The results from two comparisons show the general formation flying evolution and the effect on the mission groundtrack requirements. The evolution differences are due to the changing EO-1 state computed by the GPS receiver and Landsat-7 updates. Evolution of the ground track and the formation alongtrack, radial, and crosstrack are presented in a Landsat-7 centered rotating coordinate system with the radial direction (ordinate) being the difference in radius magnitude and the alongtrack direction (abscissa) being the arc between the position vectors. Crosstrack is a

direct measurement of cross track separation of the spacecraft which is a function the orbital plane separations necessary to meet the ground track requirement. Figures 7 and 8 present alongtrack, crosstrack, and radial, separations for two maneuver scenarios. In these plots, EO-1's initial position is located on the right side of the figure at approximately 456km and 487 km alongtrack separation. Figure 9 presents the ground tracks for these maneuver scenarios.

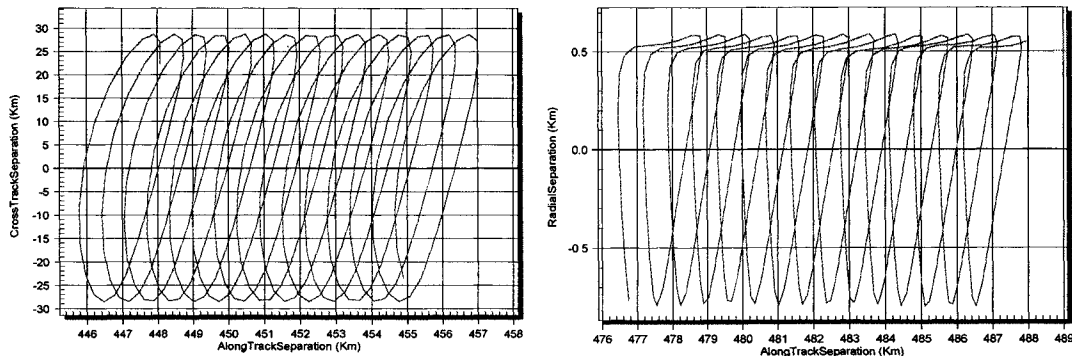


Figure 7. EO-1 Alongtrack vs. Radial Differences in a Rotating Coordinate System

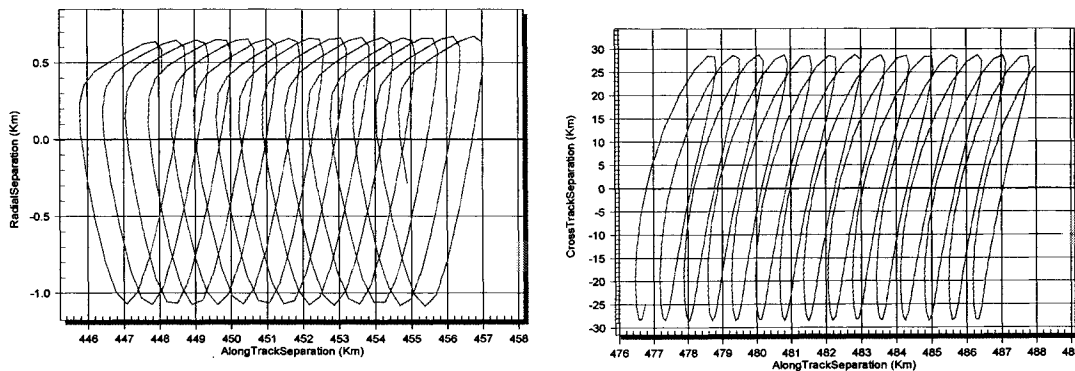


Figure 8. EO-1 Crosstrack versus Alongtrack Differences in a Rotating Coordinate System

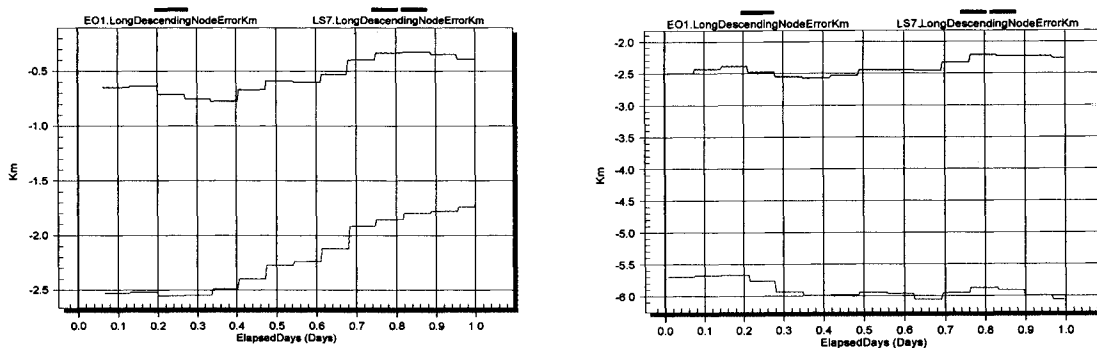


Figure 9. EO-1 and LS7 GroundTrack

### Maneuver Comparisons

This section presents onboard and ground comparison results in terms of the absolute difference in the computed  $\Delta V$  (cm/s) and the related percentage error for several maneuver scenarios. A total of 12 scenarios consisting of 3 maneuver sets (two maneuvers per set) for a total of 36 combined maneuvers were verified. The locations and epochs of these maneuvers were chosen randomly at approximately one per day over a three-week span. Figures 10 and 11 present the overall performance of each quantized maneuver as an absolute difference in the  $\Delta V$  magnitude

and its percent error. The mean value of the quantized difference is 0.0001890cm/s with a standard deviation of 0.000133 cm/s. These data show that there is excellent agreement between the onboard system and ground validation system. The larger residual in figure 10 is due to a 1-second quantization of a velocity-matching maneuver. This difference is due to the onboard system yielding a maneuver duration near the mid point which rounded down while the ground system rounded up. The difference is still small at 1.4%. The next figures, 12 and 13, present maneuver comparisons for the 3-D computation. This provides the comparisons for the total  $\Delta V$  required to align EO-1 directly behind Landsat-7 and involves all three  $\Delta V$  components of radial, alongtrack, and crosstrack.

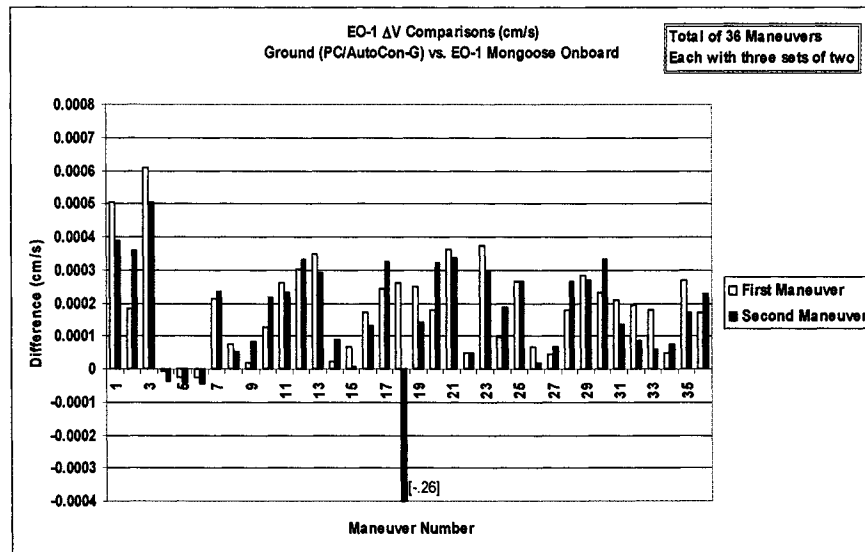


Figure 10. Difference in EO-1 Onboard and Ground Absolute  $\Delta V$ s

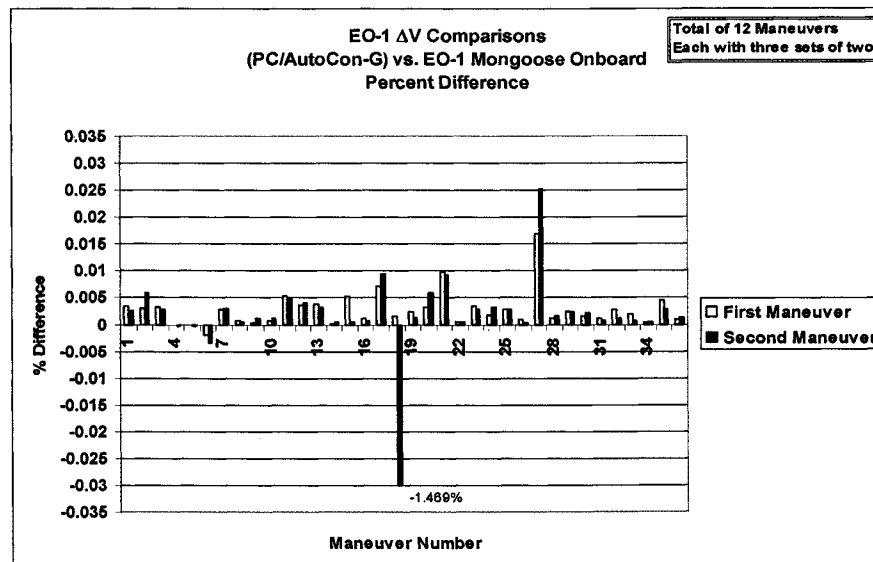


Figure 11. Percentage Difference in EO-1 Onboard and Ground Absolute  $\Delta V$ s

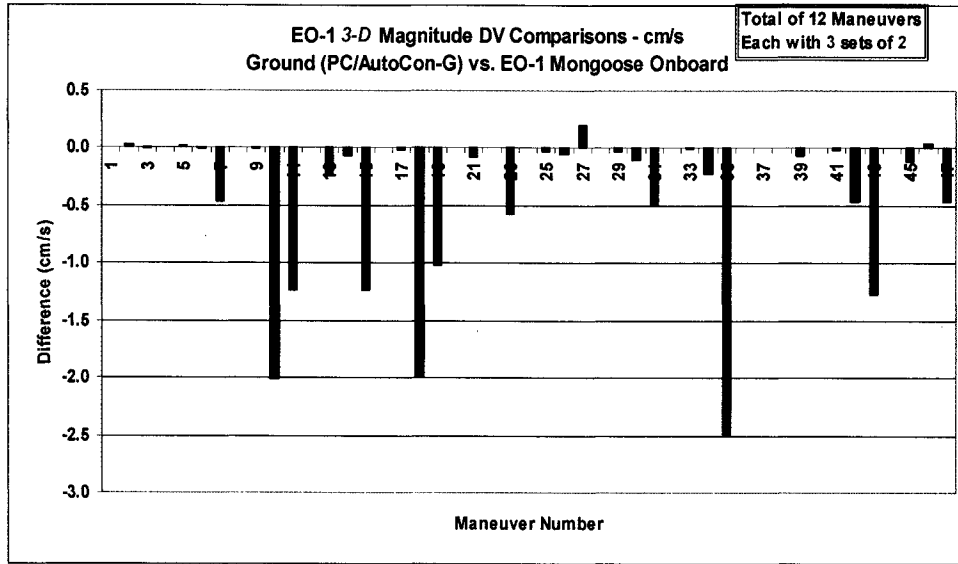


Figure 12. Absolute Difference in 3-D Onboard and Ground ΔVs

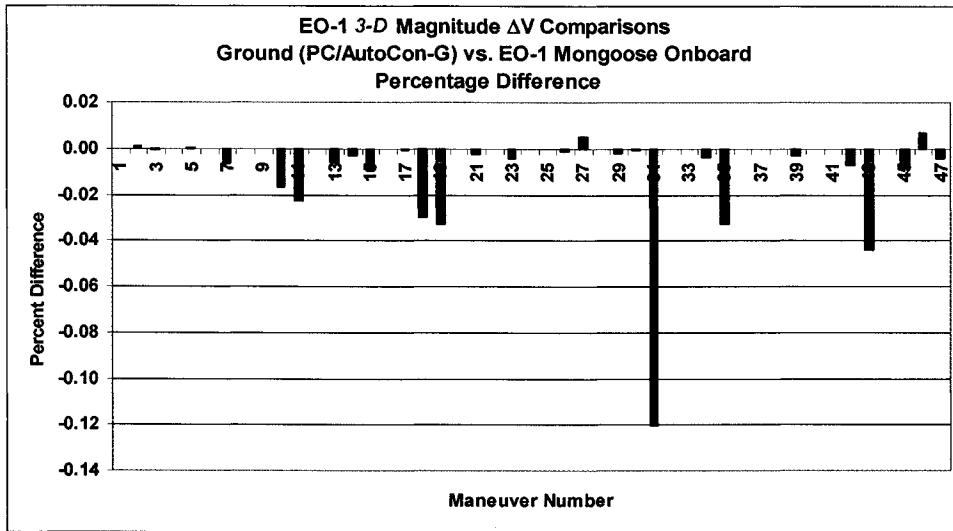


Figure 13. Percentage Difference in 3-D Onboard and Ground ΔVs

Obviously the crosstrack component is the driver with the largest magnitude. The comparisons show only the total ΔV magnitude, as this is the only information available in EO-1 playback telemetry.

With the comparisons between the ground and operational onboard version of the EFF completed, a comparison to the original FQ algorithm code was then performed. This comparison was done only for the first FQ targeted maneuver of each maneuver scenario. The state data from the playback telemetry was input into a MATLAB™ script with the FQ algorithm computing the maneuver without any propagation.<sup>3,7</sup> Figures 14 and 15 show the difference in cm/s and as a percentage respectively for the 3-D  $\Delta V$  and an alongtrack  $\Delta V$ . The alongtrack  $\Delta V$  was represented in the MATLAB™ script by using a local-vertical local horizontal coordinate system based on the input states which is comparable to the EO-1 nominal attitude for maneuvers. The resulting  $\Delta V$  difference gives a mean of 0.0727 cm/s and a standard deviation of 0.348058 for the 3-D and gives a mean of -0.03997 cm/s and a standard deviation of 0.278402 for the alongtrack. The mean percentage difference was 0.003 for the 3-D and 0.006 for the alongtrack. These results show excellent comparisons.

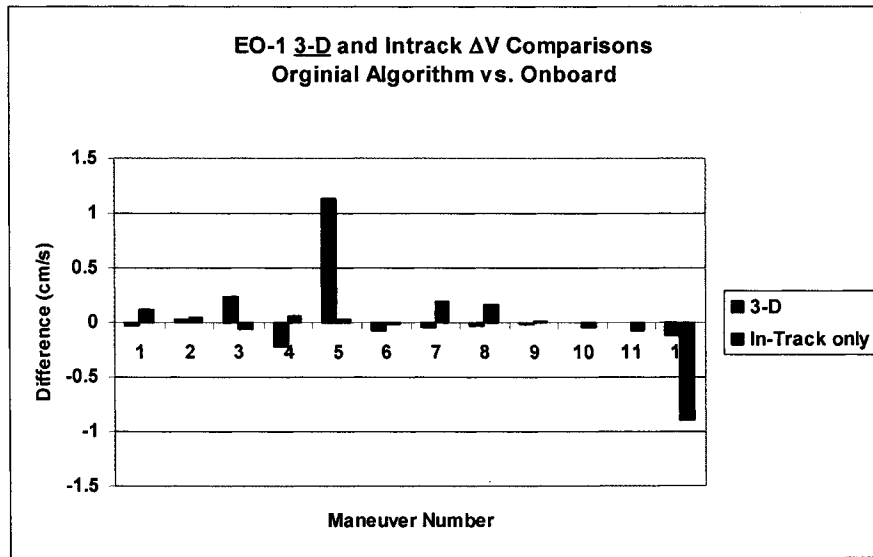


Figure 14.  $\Delta V$  Difference in Original Algorithm and Onboard

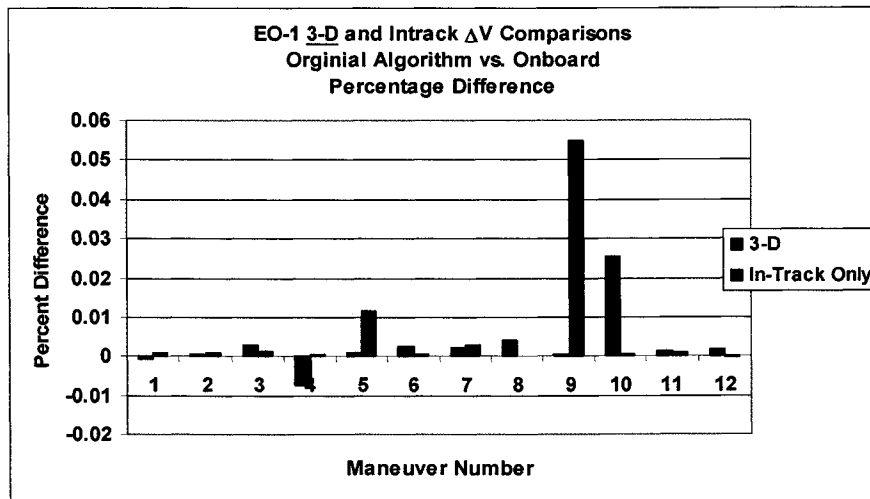


Figure 15. Percentage Difference in Original Algorithm and Onboard

## Propagation Comparisons

The FQ Algorithm is dependent upon the generation of the target and desired states. These states are propagated onboard using a Runge-Kutta 4/5 with an 8x8 Geopotential model and a Jacchia-Roberts atmospheric drag model. The accuracy of the computed  $\Delta V$  is dependent upon the accuracy of these propagated states. For EO-1, the states are propagated forward 1 and  $\frac{1}{2}$  orbits to compute the target state and then propagated 1 and  $\frac{1}{2}$  orbits backward to compute the desired state. As the desired state incorporates the longest propagation duration with a restart, a comparison was made in the onboard and ground states. The comparison results are shown below in figures 16 and 17. Figure 16 shows the position component and magnitude differences for six maneuver plans. Figure 17 shows the velocity differences. The maximum difference observed was 1.35 meters in the y-component of position and 1.4 cm/s in the velocity z-component. These small differences are still being investigated, but are believed to be the due to the integration into and performance of the EO-1 computer. The mean and standard deviations for position are listed in table 1.

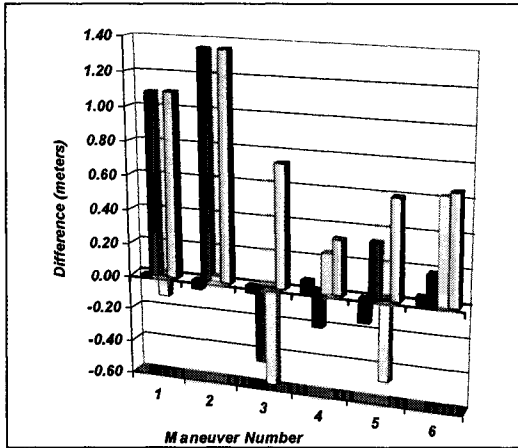


Figure 16. 1.5 Orbit Propagation Position Difference

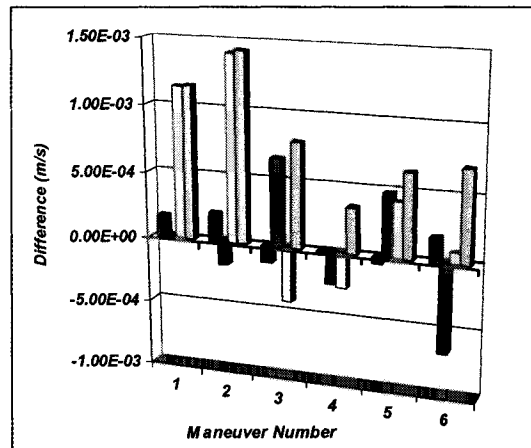


Figure 17. 1.5 Orbit Propagation Velocity Difference

Table-1. Propagation Mean and Standard Deviation for Desired State Computation

	X	Y	Z	Magnitude
Position Mean (m)	-0.02279	0.38221	-0.04550	0.79088
Position StDev (m)	0.07676	0.70684	0.45024	0.36886
Velocity Mean (m/s)	0.00007	0.00001	0.00040	0.00084
Velocity StDev (m/s)	0.00014	0.00049	0.00074	0.00039

## SUMMARY

Using the formation flying algorithms developed by the Guidance, Navigation, and Control center of GSFC, onboard validation has shown that the EO-1 formation flying requirements can be easily met. To ensure the accuracy of the onboard FQ algorithm, several comparisons were performed against both original analytical calculations and ground based FQ numerical computations using AutoCon™ for given initial onboard-generated states. The FQ algorithm was validated by direct inputs of the initial taken from the onboard system. The  $\Delta V$  results agree to millimeters/sec level for the numerical tests which include the effects of propagation. The Matlab simulations agree to the sub-cm/sec as well, due to the differences in PC and Mongoose applications.

## CONCLUSIONS

The GSFC GNCC's Folta-Quinn formation flying algorithm is a innovative technology that can be used in a closed-loop design to meet science and mission requirements of all low Earth orbiting formation flying missions. The algorithm is very robust in that it supports not only benign groundtrack control and relative separation control, but also demanding 3-D control for inclination and non-Keplerian transfers. To best meet the NMP requirements, this innovative technology is flying onboard the EO-1 spacecraft. The algorithm was successfully integrated into AutoCon™ for ground support validation, closed-loop onboard autonomy, as well as operational support. The application of this algorithm and the AutoCon™ system to other NASA programs is unlimited, as it applies to any orbit about any planet and can be used to fully explore the NASA mandate of faster, better, cheaper spacecraft.

## REFERENCES

1. Frank Bauer, David Quinn, Kathy Hartman, David Folta, and John Bristow "Enhanced Formation Flying Experiments For The New Millennium Program Earth Orbiter (EO)-1 Mission - Challenging Technology Program Management", AIAA, 5/97
2. John Bristow, David Folta, Kate Hartman, and Jessie Leitner, "A Formation Flying Technology Vision", AIAA-2000-5194, February 2000
3. David Folta and David Quinn, "A Universal 3-D Method for Controlling the Relative Motion of Multiple Spacecraft in Any Orbit," Proceedings of the AIAA/AAS Astrodynamics Specialists Conference, August 10-12, Boston, MA.
4. Quinn, D.A. and D. C. Folta (1996) *Patent Rights Application and Derivations of Autonomous Closed Loop 3-Axis Navigation Control Of EO-1.*
5. Battin, R. (1987) *An Introduction to the Mathematics and Methods of Astrodynamics*, AIAA Education Series, Chapters 9 and 11.
6. Sperling, R. (1997) *AutoCon User's Guide Version 3.0*, February 1998, AI Solutions, Inc., Greenbelt, MD. 20770
7. Matlab, The Math Works, Inc, Users Guide, 1995